Linear Time Computation of Robust Stability Margins

M. Sami Fadali
Electrical Engineering Dept./ 260
University of Nevada
Reno, NV 89557
PIN: 01807
Fadali@ee.unr.edu

Laurence E. LaForge
The Right Stuff of Tahoe, Incorporated
3341 Adler Court
Reno, NV 89503-1263
PIN: 19613
Larry@The-Right-Stuff.com

A. Sonbol
Electrical Engineering Dept./ 260
University of Nevada
Reno, NV 89557
PIN: -0239
Sonbol@ee.unr.edu

Abstract

Applying recent results for feasible regions of compensation, we introduce an optimal algorithm for computing combined phase and gain stability margins. We consider the case of a rational transfer function with independent interval uncertainty in the numerator and denominator. For any given frequency, our algorithm expresses the minimal complex perturbation that destabilizes the transfer function. We furnish an example that contrast our results with classical margins for gain and phase, as well as with the structured singular value μ

Key words: ***robust stability***; ***stability margins, value sets***

1. Introduction

Stability margins are established tools for the assessment of relative stability [5]. Traditional stability margins, the phase margin and the gain margin, provide measures of relative stability in the presence of phase or gain perturbations, respectively.

Although most engineering systems with adequate phase and gain margins perform satisfactorily, it is well known that a system can have acceptable stability margins but poor relative stability [5]. This is because the classical margins do not examine the effect of simultaneous gain and phase perturbations. A more complete assessment of relative stability is possible if both a gain and a phase perturbation are considered simultaneously. This more general perturbation is harder to analyze but does offer significant advantages.

We show that if line segments and circular arcs constitute the boundary of the reciprocal Nyquist value set of a transfer function, and if those segments and arcs are known, then the complex stability margin can be easily determined. Repeating the process at different frequencies provides a set of complex stability margins for use in stability analysis. The prerequisite step for implementing such a procedure is the computation of the required line segments and circular arcs. However, the much more difficult task of calculating the reciprocal Nyquist value set is not required. Nevertheless, knowledge of the Nyquist value set sheds light on our objective. We therefore review the literature on Nyquist value set computation.

The Nyquist or reciprocal Nyquist value set of the quotient of two interval polynomials is a complex uncertainty structure, and its computation is somewhat more intricate than that in the case an interval polynomial. Several authors have provided algorithms that use gridding to compute the quotient value set [2],[6]. Others have attempted to compute the convex hull of the value set or provided iterative algorithms for obtaining less conservative estimates of the value set [16].

Fu [12] sketches a superexponential algorithm for computing the Nyquist value set. Recently, Cockburn *et al.* [6] introduce applications of computational geometry [15] to the problem of explicating the value set boundary. Independently, and bolstering research reported in [9], Fadali and LaForge exploit techniques from computational geometry to derive an optimal, linear time algorithm [8] that computes the Nyquist value set or its reciprocal [10]. Both the Nyquist value set and its reciprocal may be viewed as *Minkowski quotients*.

For rational transfer functions, the cost of computing the Nyquist value set boundary is dominated by the degree of the interval polynomials comprising numerator and denominator [10]. By combining Horner's Rule with the Dasgupta-Minichelli form of Kharitonov's theorem, Fadali and LaForge solve this subproblem with an optimal algorithm: **Kharitonov-Rectangle** ([10], Sections 2 and 3). **Kharitonov-Rectangle** outputs edges that prescribe the value sets of the plant transfer function numerator *resp.* denominator. From this stage on, the problem of delineating the Nyquist value set (or its reciprocal) reduces to finding the boundary of the 16 arcs and 16 edges determined by dividing the corners of each rectangle by the edges of the other ([10], Lemma 2). **Q-Boundary** is an optimal, constant time algorithm that performs this task. The number of distinct portions of **Kharitonov-Rectangle** and edges and arcs on the Nyquist set boundary is bracketed by a constant, and under no circumstances exceeds 480 ([10], Theorem 2).

In this paper we develop a new optimal algorithm that computes robust stability margins for a transfer function with numerator and denominator interval polynomials. Estimates of the stability margin for more complex uncertainty structures can be obtained by overbounding the polynomials [1], [3]. By this we mean replacing the uncertain polynomials with interval polynomials that overbound their value sets. Although this may give conservative estimates, it still provides useful information about the relative stability of the system.

Under certain conditions, the results we obtain can be applied to multivariable systems. For the case of diagonally dominant multivariable systems, the above analysis can be applied to each loop separately to yield stability robustness estimates. An alternative approach is to use a little known theorem due to Rosenbrock [14] that reduces p-loop multivariable stability testing to the sequential testing of p single-input, single-output (SISO) systems.

We also show how, at any given frequency, determining the *structured singular value* m reduces to finding the minimum magnitude point in the reciprocal Nyquist value set. Suppose that we have already used **Q-Boundary** to compute the arcs or edges comprising the reciprocal Nyquist set boundary. By considering each arc or edge on this boundary, we can find the minimum magnitude point in constant time. If, on the other hand, we do not require an explicit formulation of the reciprocal Nyquist set, then a somewhat simpler algorithm, **SSV** (*Structured Singular Value*) suffices. In optimal time proportional to the degree of the dominant polynomials, **SSV** maps the outputs of **Kharitonov-Rectangle** into 16 arcs and 16 edges ([10], Lemma 2), thence to the minimum magnitude point.

We begin the paper with a discussion of the Nyquist value set for a rational transfer function with independent numerator and denominator interval polynomials. Next, we discuss the complex stability margin and its computation using the algorithm Q-Boundary. We provide illustrative examples to show the limitations of other stability criteria.

2. The Nyquist Value Set

Consider the closed-loop transfer function of Figure 1

$$T(s) = \frac{Y_{\text{out}}(s)}{Y_{\text{in}}(s)} = \frac{\Delta(s)P(s)}{1+\Delta(s)P(s)} \qquad (1)$$

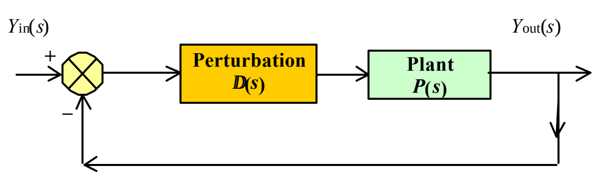

Figure 1: Feedback loop illustrating system components and their respective transfer functions.

To determine important characteristics of the closed-loop transfer function it is necessary to examine the plant transfer function. Here, the plant transfer function refers to all transfer functions excluding the unstructured perturbation $D(s)$. The plant transfer function $P(s)$ is the ratio of a numerator polynomial $A(s)$ of degree m and a denominator polynomial $B(s)$ of degree n, $n \geq m$:

$$A(s) = \sum_{k=0}^{m} a_k\, s^k \qquad B(s) = \sum_{k=0}^{n} b_k\, s^k \qquad (2)$$

The $m+n+2$ coefficients $\{a_0, \ldots, a_m\} = \boldsymbol{a}$ and $\{b_0, \ldots b_n\} = \boldsymbol{b}$ are functions of the physical parameters of the plant. We assume that a real interval $[a_k^-, a_k^+]$ contains the k^{th} coefficient a_k, for $0 \leq k \leq m$, and a real interval $[b_k^-, b_k^+]$ similarly brackets each b_k. We denote the two families of uncertain polynomials by:

$$A^{\square}(s) = \sum_{k=0}^{m} [a_k^-, a_k^+] \cdot s^k, \;\; B^{\square}(s) = \sum_{k=0}^{n} [b_k^-, b_k^+] \cdot s^k \qquad (3)$$

We write $A^{\square}(jw)$ and $B^{\square}(jw)$ for the value sets of the interval polynomials $A(s)$ and $B(s)$ at a given frequency. The value sets of interval polynomials are described by Kharitonov's Theorem [3], [13].

Theorem 1. The value sets of the interval polynomials **(3)** are rectangles (5) - (8) in the complex plane.

Theorem 1 reduces uncertainty in $(m+1)$ *resp.* $(n+1)$ dimensions to rectangles with sides paralleling the abscissa and ordinate. Figure 2 gives an example of the Kharitonov rectangles for the numerator and denominator polynomials.

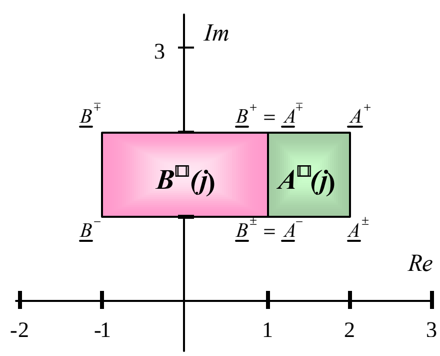

Figure 2: Kharitonov rectangles:
$A^{\square}(j1) = [1, 2]\, s + [1, 2]$, $B^{\square}(j1) = [1, 2]\, s^2 + [1, 2]\, s + [1, 2]$.

In **(2)** replace a_k or b_k with one end of the corresponding interval in according to

$$A_i(s) = \sum_{k=0}^{m} a_k^{\ell} \cdot s^k, \;\; B_i(s) = \sum_{k=0}^{n} b_k^{\ell} \cdot s^k, \; i = 1,2, \ldots, 4,$$

if k mod 4 $\in \{0,1\}$, then $\ell = -$, else $\ell = +$ (4)

At any frequency $w = w_0$, the *Kharitonov polynomials* (4) determine lines parallel to the real and imaginary axes:

$$A_{\text{Re}}^{\,-}(jw_0) = \text{Re}[\underline{A}_1(jw_0)],$$
$$B_{\text{Re}}^{\,-}(jw_0) = \text{Re}[\underline{B}_1(jw_0)] \qquad (5)$$

$$A_{\mathrm{Re}}^{+}(jw_0) = \mathrm{Re}[\underline{A}_2(jw_0)] \; B_{\mathrm{Re}}^{+}(jw_0) = \mathrm{Re}[\underline{B}_2(jw_0)] \tag{6}$$

$$A_{\mathrm{Im}}^{-}(jw_0) = \mathrm{Im}[\underline{A}_3(jw_0)], \quad B_{\mathrm{Im}}^{-}(jw_0) = \mathrm{Im}[\underline{B}_3(jw_0)] \tag{7}$$

$$A_{\mathrm{Im}}^{+}(jw_0) = \mathrm{Im}[\underline{A}_4(jw_0)], \quad B_{\mathrm{Im}}^{+}(jw_0) = \mathrm{Im}[\underline{B}_4(jw_0)] \tag{8}$$

In clockwise order, $(A_{\mathrm{Re}}^{-}, A_{\mathrm{Im}}^{-}) = \underline{A}^{-}$, $(A_{\mathrm{Re}}^{-}, A_{\mathrm{Im}}^{+}) = \underline{A}^{\mp}$, $(A_{\mathrm{Re}}^{+}, A_{\mathrm{Im}}^{+}) = \underline{A}^{+}$, and $(A_{\mathrm{Re}}^{+}, A_{\mathrm{Im}}^{-}) = \underline{A}^{\pm}$ define the corners of the rectangle whose boundary *and* interior comprise $A^{\square}$. Similarly, the extrema of $B^{\square}$ are $(B_{\mathrm{Re}}^{-}, B_{\mathrm{Im}}^{-}) = \underline{B}^{-}$, $(B_{\mathrm{Re}}^{-}, B_{\mathrm{Im}}^{+}) = \underline{B}^{\mp}$, $(B_{\mathrm{Re}}^{+}, B_{\mathrm{Im}}^{+}) = \underline{B}^{+}$, and $(B_{\mathrm{Re}}^{+}, B_{\mathrm{Im}}^{-}) = \underline{B}^{\pm}$. Barmish ([3], pp. 70-73) gives a very accessible proof of Theorem 1.

Interval polynomials and their properties are extensively discussed, together with other uncertainty structures, in excellent texts covering the subject of robust stability [1],[3]. Here we are more concerned with the quotient of two interval polynomials.

Rewriting the transfer function of (1) in terms of the interval polynomials gives

$$T^{-1}(s) = P^{-1}(s) + C(s) = \frac{B^{\square}(s)}{A^{\square}(s)} + C(s) \tag{9}$$

The reciprocal of a straight line segment is known to be a circular arc, excluding the origin, of a circle passing through the origin [1]. Hence, the Nyquist value set or its reciprocal are characterized by the following lemma [10].

Lemma 1: The boundary of $P^{-1\square}$ is a subset of the sixteen circular arcs and sixteen edges formed by dividing each of: (i) the four corners of $-B^{\square}$ by each of four edges of $A^{\square}$(16 arcs), (ii) the four edges of $-B^{\square}$ by each of four corners of $A^{\square}$ (16 segments).

Lemma 1 characterizes the boundary of the Minkowski quotient in terms of 16 arcs and 16 line segments. The boundary of $P^{-1\square}$ is complex because of the wide variety of combinations of the 16 arcs and edges possible. The vertices of $P^{-1\square}$ include intrinsic vertices of the arcs and edges as well as nonintrinsic vertices resulting from the arc-edge intersections. Q-boundary allows us to find the nonintrinsic edges and construct the boundary of $P^{-1\square}$. We exploit this in the next section to determine the relative stability of a plant with interval numerator and denominator.

3. Complex Stability Margin

A multiplicative perturbation $D(s)$ can result in significant deterioration in the performance of the closed-loop system of Figure 1 and may even result in instability. We seek the set of complex perturbations that cause closed-loop instability at a given frequency and for a given point on the boundary of the Nyquist value set corresponding to a parameter vector $\boldsymbol{q}_b$. We refer to the destabilizing perturbations as the *complex stability margin*. The complex stability margin is therefore given by

$$CM(jw, \mathbf{q}_b) = \left\{ \begin{matrix} \Delta(jw) = M(w)e^{jf(w)} : \\ 1 + \Delta(jw) \cdot P(jw, \mathbf{q}_b) = 0 \end{matrix} \right\} \tag{10}$$

Solving for the minimal perturbation gives

$$CM(jw, \boldsymbol{q}_b) = -\frac{1}{P(jw, \boldsymbol{q}_b)} \tag{11}$$

Clearly, a boundary for the region of destabilizing perturbations at a given frequency is the negative of the boundary of the reciprocal Nyquist value set. Hence, we can use the algorithm Q-Boundary to determine the complex stability margin at any desired frequency. The interior of this boundary is the region of destabilizing perturbations for the plant. Any perturbation outside this region no matter how large will not destabilize the plant. Because we do not consider nonminimum phase systems, our analysis preclude cases where the outside of the boundary is the region of destabilizing perturbations.

4. Relation to *m* Analysis

For the system of Figure 1, the smallest destabilizing perturbation for the system is given by [11]

$$\min_{w, \Delta(jw)} \left\{ M(w) : 1 + \Delta(jw) \cdot P(jw, \mathbf{q}) = 0 \right\} \tag{12}$$

where we have modified the equation for the SISO case we consider in this paper. A system is said to be robustly stable if and only if the smallest destabilizing perturbation exceeds unity. Note that in our analysis we allow for a structured perturbation in the parameter vector $\boldsymbol{q}$ as well as a multiplicative perturbation D.

The structured singular value is defined as the reciprocal of the smallest destabilizing perturbation

$$m = \frac{1}{\min_{D(jw)} \left\{ M(w) : 1 + D(jw) \cdot P(jw, \boldsymbol{q}) = 0 \right\}} \tag{13}$$

It is well known that the computation of the structured singular value is intractable except for a few simple cases. A stronger negative result due to Fu [11] shows that computing tight bounds on the structured singular value is also intractable, in general.

Comparing (13) to (10) shows that the structured singular value is simply

$$m = \max_{w} CM(jw, \mathbf{q}_b) \tag{14}$$

Hence, the structured singular value can be obtained by searching over the boundary of the reciprocal Nyquist value set for the point of minimum magnitude. The algorithm for computing the structured singular value is

Algorithm SSV (Structured Singular Value)
Input: upper and lower bounds for each coefficient of the transfer function $P = A/B$. The degree of A equals m; and is no greater than the degree n of B.

1) Use **Kharitonov-Rectangle-A** to compute, in time $O(m)$, the Kharitonov rectangle for A.
2) Use **Kharitonov-Rectangle-B** to compute, in time $O(n)$, the Kharitonov rectangle for B.
3) Compute (in, say, convex parametric form) the 16 arcs and 16 edges of [10], Lemma 2. Time: $O(1)$
4) Over all such arcs and edges, and in time $O(1)$ find the closest point to the origin. The magnitude of this point equals the reciprocal of the structured singular value.

Algorithm SSV does not check for minimum distance on a circular arc. The special nature of the circular arcs that form part of the boundary of the reciprocal Nyquist set guarantees that the minimum distance is at a vertex.

Lemma 2. The minimum distance from the origin over all points of a circular arc obtained as the reciprocal of a straight line segment is at a vertex.

Proof: Consider the circle obtained as the reciprocal of a straight line shown in Figure 3. Any such circle must pass through the origin. The distance from the origin for any point on the circle is the length of the line segment subtending the arc from the origin to that particular point. Compare two adjacent point on the segment between vertices $V[1]$ and $V[2]$ and recall the cosine rule. We conclude that the closest point to the origin among all points on an arc of the circle is the point with the shortest arc from the origin.

♦

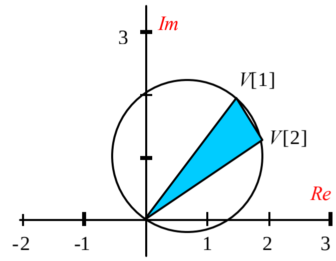

Figure 3: **Circle from the reciprocal of a straight line.**

It follows that the algorithm SSV correctly computes the structured singular value for a system with structured and mulitplicative perturbations.

Theorem 2. Algorithm SSV correctly computes the structured singular value in optimum time $\mathbf{\Theta(n)}$.

Proof: The correctness of **SSV** follows from the correctness of **Kharitonov-Rectangle**, from Lemma 2 of [10], and by the definition of structured singular value. The $O(n)$ running time follows by summing the running times of the respective steps, with some detail (but constant time computation) omitted in step 4. With respect to a Turing machine model of computation, **SSV** runs in optimal time $\Theta(n)$: any algorithm that solves for the structured singular value must read the $\Omega(n)$ representation of the polynomial input.

♦

5. Extension to Multivariable Stability Analysis

Rosenbrock [14] discussed testing multivariable system stability using a series of SISO stability tests. His discussion includes the following theorem [14].

Theorem 3. Consider a p-input-p-output systems with p feedback loops numbered i =1,2, …, p. The closed-loop characteristic polynomial of the system with p feedback loops closed is equal to the product of the characteristic polynomials of the systems h_i, i =1,2, …, p, where the ith system is obtained by closing loops 1,2, …, i, with all the other loop open.

Using the above theorem, it is possible to extend the robust stability analysis of Section 4 to multivariable systems. We begin by investigating the stability of loop 1 with all other loops closed. Next, we close loop 1 and investigate the stability of loop 2. We continue sequentially until $p-1$ loops are closed and the stability of the pth loop is investigated.

6. Example and Discussion

Consider the uncertain system

$$P(s) = \frac{[1,2]s + [1,2]}{[1,2]s^2 + [1,2]s + [1,2]}$$

We take the nominal model for the system as the point corresponding to the lower bound of the uncertainty interval for each of the numerator and denominator coefficients. This point yields the worst-case phase and gain margins for the system.

Figure 4 shows the magnitude of the minimal destabilizing perturbation for the system as a function of frequency. The minimum destabilizing perturbation over all frequencies is of magnitude 0.2801 at a frequency 0.6400 rad/s. The corresponding structured singular value is *m* = 3.5702 For the nominal system, the gain margin is not defined and the phase margin is about 110°. This gives an overly optimistic view of the relative stability of the system as compared to the structured singular value *m*

Figure 5 shows the set of destabilizing perturbations for a frequency of 0.64 rad/s (interior of quasi-polygon), and the negative of the nominal plot of $-P^{-1}$ for a suitable frequency grid. The magnitude of the smallest destabilizing real perturbation is only 0.5 even though the gain margin of the nominal system is infinite. We include the arcs and segments that constitute the boundary in Figure 5 even though the algorithm Q-boundary computes the boundary. SSV uses the shown line segments and arcs to compute the structured singular value. The algorithm considers the distance from the origin of at least two and at most three points on each line segment and each circular arc. Clearly, the computation of the reciprocal Nyquist value set by Q-boundary is not required for SSV.

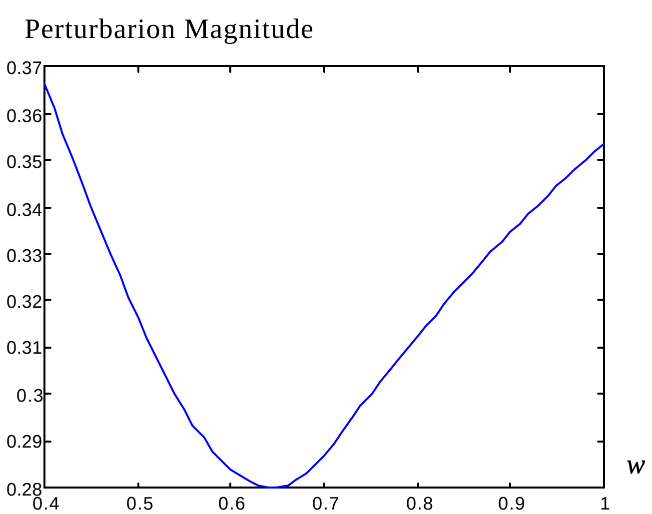

Figure 4. Plot of the magnitude of the minimal destabilizing perturbation versus frequency in rad/s.

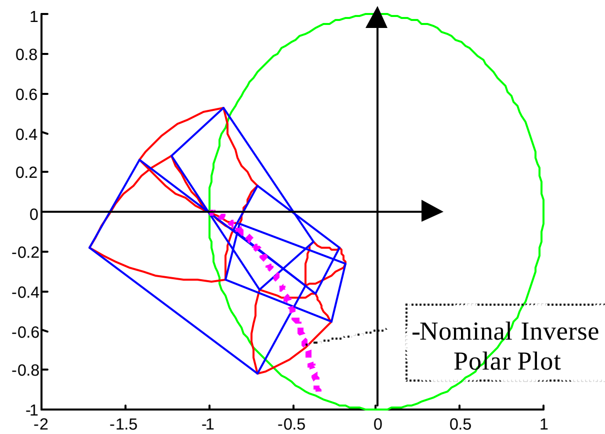

Figure 5. Set of destabilizing perturbations at *w*=0.64 and $-P^{-1}$ plot for the nominal system.

7. Conclusion

While the stability of the nominal linear model of a physical system can be conveniently investigated using classical frequency domain criteria, the stability of systems with parametric and nonparametric perturbations is more problematic. This paper examines the stability of perturbed systems guided by a new algorithm to compute the reciprocal Nyquist value set for the ratio of two interval polynomials and the structured singular value. The investigation shows that traditional stability margins can give misleading relative stability predictions. The structured singular value improves the quality of the predictions. The computation of the structured singular value, which is known to be intractable in general, is shown to be tractable for the case of a rational transfer function with interval numerator and denominator. Similarly, we can compute upper and lower bounds on the H^∞ norm for the same case. Contrary to statements in the literature [12], we emphasize that both *m* and the H^∞ norm can be computed **without the computation of the Nyquist value set**.

The algorithm presented here promises further results for robust stability computations. With some modifications, the algorithm developed in this paper can be used for transfer function where the boundary of the Nyquist value set consists of line segments and circular arcs, other than those with interval uncertainty structure.

Another important extension is the calculation of the real structured singular value (real *m*). We have developed a linear time algorithm for real *m* computation for the case of interval polynomial numerator and denominator. Again, the computation of real *m* like its complex counterpart, does not require the computation of the Nyquist value set. These topic are beyond the scope of this paper but will be presented in forthcoming papers.

References

[1] J. Ackermann. *Robust Control: Systems with Uncertain Physical Parameters*. London: Springer-Verlag, 1993.

[2] F. N. Bailey and C.-H. Hui. A fast algorithm for computing parametric rational functions. *IEEE Transactions on Automatic Control*. **34** (11), November, 1989. pp. 1209-1212.

[3] B. R. Barmish. *New Tools for Robustness of Linear Systems*. New York: Macmillan Publishing, 1994.

[4] A. C. Bartlett. Nyquist, Bode, and Nichols plots of uncertain systems. *Proceedings, 1990 ACC*. San Diego: May, 1990. Vol. 2, pp 2033 - 2036.

[5] P. R. Bélanger. *Control Engineering: A Modern Approach*. Montreal: Saunders, 1995.

[6] J. C. Cockburn and M. A. Lopez. Geometric computation of value set boundaries. *Proc.2000 ACC*. Chicago: June, 2000. pp. 4326-4330.

[7] B. Cohen, M. Nordin, and P.-O. Gutman. Recursive grid method to compute value sets for transfer functions with parametric uncertainty. *Proc. 1995 ACC*. Seattle: 1995. pp. 3861-3865

[8] T. H. Cormen, C. E. Leiserson, and R. L. Rivest. *Introduction to Algorithms*. NY: McGraw Hill, 1993.

[9] M. S. Fadali and L. E. LaForge. Algorithmic analysis of geometrically computed QFT bounds. *In Proc. IFAC World Congress*, **H.** San Francisco, June, 1996. pp. 297-302.

[10] M. S. Fadali and L. E. LaForge. Linear time computation of feasible regions for robust Compensators. *J. Robust and Nonlinear Control*, (to appear 2001).

[11] M. Fu. The real structured singular value is hardly approximable. *IEEE Transactions on Automatic Control*. **42** (9), September, 1997. pp. 1286-1288.

[12] M. Fu. Computing the frequency response of linear systems with parametric perturbation. *Systems and Control Letters*. **15** (1), 1990. pp. 45 - 52.

[13] V. L. Kharitonov. Asymptotic stability of an equilibrium position of a family of systems of linear differential equations. *Differentsial'nye Uravneniya*, Vol 14, 1978. pp 2086-2088. English translation in *Differential Equations*, Vol 14, 1978. New York: Plenum Publishing. pp 1483-1485.

[14] H. H. Rosenbrock, *Computer Aided Control System Design*, Academic Press, London, 1974.

[15] F. P. Preparata, M. I. Shamos. *Computational Geometry: an Introduction*. New York: Springer-Verlag. 1985.

[16] B. H. Wilson, B. Eryilmaz, and B. Shafai. An adaptive angular sweep algorithm for value set construction. *IEEE Transactions on Automatic Control*. **44** (3), March, 1999. pp. 551-555.